Basic reproduction number for pandemic *Escherichia coli* clones varies markedly and can be comparable to pandemic influenza viruses

Fanni Ojala[1†], Henri Pesonen[2†], Rebecca A. Gladstone[3], Tommi Mäklin[4], Gerry Tonkin-Hill[3,5,6,7], Pekka Marttinen[1†], Jukka Corander[3,4,8,9*†]

[1]Department of Computer Science, Aalto University, Konemiehentie 2, Espoo, 02150, Finland.
[2]Oslo Center for Biostatistics and Epidemiology, Oslo University Hospital, Sognsvanssveien 9, Oslo, 0372, Norway.
[3]Department of Biostatistics, University of Oslo, Sognsvanssveien 9, Oslo, 0372, Norway.
[4]Helsinki Institute for Information Technology HIIT, Department of Mathematics and Statistics, University of Helsinki, Yliopistonkatu 3, Helsinki, 00014, Finland.
[5]Peter MacCallum Cancer Centre, 305 Grattan Street, Melbourne, 3000, Australia.
[6]Sir Peter MacCallum Department of Oncology, The University of Melbourne, Grattan Street, Melbourne, 3010, Australia.
[7]Department of Microbiology and Immunology, The University of Melbourne at the Peter Doherty Institute for Infection and Immunity, 792 Elizabeth Street, Melbourne, 3000, Australia.
[8]Parasites and Microbes, Wellcome Sanger Institute, Wellcome Genome Campus, Hinxton, Cambridgeshire, CB10 1SA, United Kingdom.
[9]Department of Genetics, University of Cambridge, Downing Street, Cambridge, CB2 3EH, United Kingdom.

*Corresponding author(s). E-mail(s): jukka.corander@medisin.uio.no;
Contributing authors: fanni.ojala@aalto.fi;
henri.pesonen@medisin.uio.no; r.a.gladstone@medisin.uio.no;

tommi.maklin@helsinki.fi; gerry.tonkin-hill@medisin.uio.no;
pekka.marttinen@aalto.fi;
†These authors contributed equally to this work.

Abstract

Extra-intestinal pathogenic *Escherichia coli* (ExPEC) ubiquitously colonize the human gut and represent clinically the most significant bacterial species causing urinary tract infections and bacteremia in addition to contributing to meningitis in neonates. During the last two decades, new *E. coli* multi-drug resistant clones such as ST131, particularly its clades C2 and C1, have spread globally, as has their generally less resistant sister clade ST131-A. Phylodynamic coalescent modeling has indicated exponential growth in the populations corresponding to these clades during the early 2000s. However, it remains unknown how their transmission dynamics compare to viral epidemics and pandemics in terms of key epidemiological quantities such as the basic reproduction number ($\boldsymbol{R_0}$). Estimation of $\boldsymbol{R_0}$ for opportunistic pathogenic bacteria poses a difficult challenge compared to viruses causing acute infections, since data on *E. coli* infections accumulate with a much longer delay, even in the most advanced public health reporting systems. Here, we developed a compartmental model for asymptomatic gut colonization and onward transmission coupled with a stochastic epidemiological observation model for bacteremia and fitted the model to annual Norwegian national *E. coli* disease surveillance and bacterial population genomics data. Approximate Bayesian Computation leveraged by the ELFI software package was used to infer $\boldsymbol{R_0}$ for the pandemic ST131 clades. The resulting $\boldsymbol{R_0}$ estimates for ST131-A and ST131-C2 were 1.47 (1.31-1.60) and 1.13 (1.08-1.20), respectively, indicating that the ST131-A transmission potential is comparable to pandemic influenza viruses, such as H1N1. The significantly lower transmissibility of ST131-C2 suggests that its global dissemination has been aided by antibiotic selection pressure and that it may be more effectively transmitted through health care facilities instead of primarily community driven transmission. In summary our results provide a fundamental advance in understanding the transmissibility of these opportunistic pathogens and that it can vary markedly even between very closely related *E. coli*.

Keywords: Bacterial transmission, Bloodstream infections, Basic reproduction number, *Escherichia coli*

1 Introduction

As evidenced by extensive research on emerging pathogens over the last couple of decades, such as Ebola, H1N1 influenza, SARS, MERS and SARS-CoV-2, epidemiological modeling of their transmission rates provides a key piece of information that serves many purposes, including the forecasting of future spread and design of interventions. For a critical overview of different methods for inferring R_0, and their reliability, see [1–5]. Different compartmental models can be used to model the

spread of an infectious disease in a population, out of which the most basic one is the Susceptible-Infected-Recovered (SIR) model (for details see the above references). For emerging pathogenic viruses the incubation period tends to be short, typically a matter of days, which translates to an opportunity to trace and count cases by reporting symptomatic individuals in a population on a given day or week of an ongoing epidemic. These data represent the most fundamental information needed in modeling the spread of the pathogen in such a setting, irrespective of whether deterministic or stochastic models are considered. For bacteria the situation is much more complicated and consequently R_0 is rarely inferred. The notable exceptions where R_0 has been estimated are highly virulent bacteria causing local outbreaks, such as *Neisseria meningitidis* [6] and TB [7], or bacterial strains in more closed ecological settings such as animal production facilities where their spread can be traced for example using seroconversion data [8]. Outside particularly vulnerable populations, e.g. hospital patients, common opportunistic pathogenic bacteria are frequently carried asymptomatically, potentially for months or years, and reports of infections caused by them can occur with a considerable time lag after the colonization event. Therefore determining the length of time between the acquisition of the pathogen to an infection or transmission is not feasible even in the most advanced and systematic public health surveillance systems.

Bacteria causing "hidden" pandemics can be broadly categorized into two distinct types, those which are strongly associated with nosocomial infections and are mainly spread through healthcare networks and those which predominantly spread in the community as part of the commensal microbiota of the gut, skin or the nasopharynx [9, 10]. Extra-intestinal pathogenic *Escherichia coli* (ExPEC) represent the latter category and are among the clinically most significant causes of human bacterial infections, such as bacteremia and urinary tract infections [11]. During the last decades several so-called pandemic clones of ExPEC have emerged and these are typically characterized by both high levels of virulence and antibiotic resistance [12, 13]. For two particularly famous clades belonging to the pandemic ST131 clone, ST131-A and ST131-C2, previous work has inferred the timing and rates of their expansions using a Bayesian phylodynamic approach which provides an estimate of the effective population over time [14]. Using systematic genomic surveillance of *E. coli* bloodstream infections (BSIs) in Norway over 2002-2017, it was shown that these clones likely expanded in parallel in the host population around early 2000s but also that ST131-A appeared to have markedly higher dissemination success than ST131-C2. In contrast, based on phylodynamics the clade ST131-B had already expanded much earlier in the 1990s, while ST131-C1 clade lacked evidence of a rapid exponential growth in comparison to ST131-A and ST131-C2. In summary, these results put forward ST131-A and ST131-C2 clades as attractive targets for epidemiological modeling to try to quantify their transmission efficiencies relative to each other and in a broader content in comparison with other microbes exhibiting pandemic spread.

Since systematic surveillance of asymptomatic colonization rates of *E. coli* clones has been missing, it has not been possible to turn the disease surveillance data into

similar epidemiological insight as captured by R_0. Recently, an advance in this direction was made by Mäklin et al. who inferred strain-level colonization competition dynamics from shotgun metagenomics data for a large neonatal birth cohort in the UK and for several bacterial pathogens, including *E. coli* [15]. By combining these data with temporally matched genomic *E. coli* disease surveillance from the UK, it was possible to infer the relative success of colonization vs infection for the ST131 clades [16]. Further, this information can be merged with the comprehensive population level bloodstream infection statistics available for Norway and the annual incidences of ST131-A and ST131-C2 in Norway based on the published genomic surveillance results. Here, we harness the unique opportunity presented to us by the combination of these data, and develop a compartmental model for the asymptomatic colonization and transmission of these two *E. coli* clades of ST131 in Norway and couple this with a stochastic observation model for bloodstream infections, to estimate R_0 using simulation-based inference. Comparison of their values provides useful epidemiological insight and allows relating them more directly to other pandemic pathogens in terms of the rate of their spread.

2 Results

In order to link the asymptomatic spread of *E. coli* in the host population with the reported bloodstream infections from the national surveillance in Norway, we developed a hybrid model with both a deterministic and a stochastic component. The model structure is illustrated in Figure 1. Our model consists of an unobserved compartmental SIR-like colonization model for the host population at the national level and an observation model which links the colonization with observed annual bloodstream infection incidence for clades A and C2. The observation model further uses clade-specific estimated odds ratios of causing a bloodstream infection. These odds ratios compare the frequency of asymptomatic colonization to the frequency of bloodstream infection in a temporally and geographically matched host population (UK) from which data based on representative sampling of hosts were available [15],[16]. Full details of the model are provided in the Methods section.

Figure 2 shows the marginal and joint posterior distribution of the basic reproduction number R_0 and the net transmission rate for the two *E. coli* ST131 clades. Posterior distributions of the corresponding R_0 parameters are visualized in the leftmost panel of Figure 2. Posterior means, medians and 95% posterior credible intervals for the three parameters are presented in Table 1. The posterior distributions indicate a significantly higher R_0 for clade A, translating to markedly better transmission efficiency in the underlying population.

The model fit to data and the 50/95% credible intervals for predicted BSI counts are visualized in Figure 3, showing that the hybrid model structure adequately captures the major differences between the two clades.

Figure 4 visualizes the distribution of predicted weekly colonization counts in a population of 1 000 000 individuals, with parameters τ, R_0 and Δ integrated out

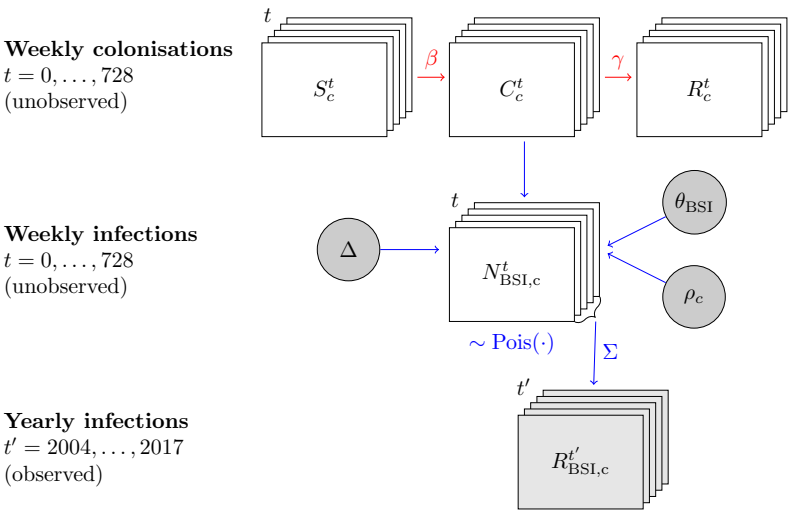

Fig. 1 Model structure. The first row shows the latent population colonization model, implemented by simulating outcomes from a compartmental SIR-like model. The compartments S_c^t, C_c^t and R_c^t are the numbers of susceptible, colonized, and removed individuals in week t for clade c. The transmission coefficient β and the recovery rate γ describe the flow between the compartments and in our implementation, the model is parametrized in terms of the basic reproduction number and net transmission rate, see [17]. The observation model is visualized below the colonization model, comprising the weekly simulated BSI counts $N_{\mathrm{BSI,c}}^t$ with the aggregated yearly BSI infection counts $R_{\mathrm{BSI,c}}^{t'}$, for which observed values are available from the national surveillance system. In the observation part, parameter ρ_c is the estimated relative invasiveness of clade c, θ_{BSI} is the fraction of the population experiencing an *E. coli* BSI caused by any clade and Δ specifies the number of years simulated colonization processes precede the observed data, essentially representing an expected time lag between colonization and infection. A Poisson observation model is used to invoke stochastic variation in the simulated BSI case counts.

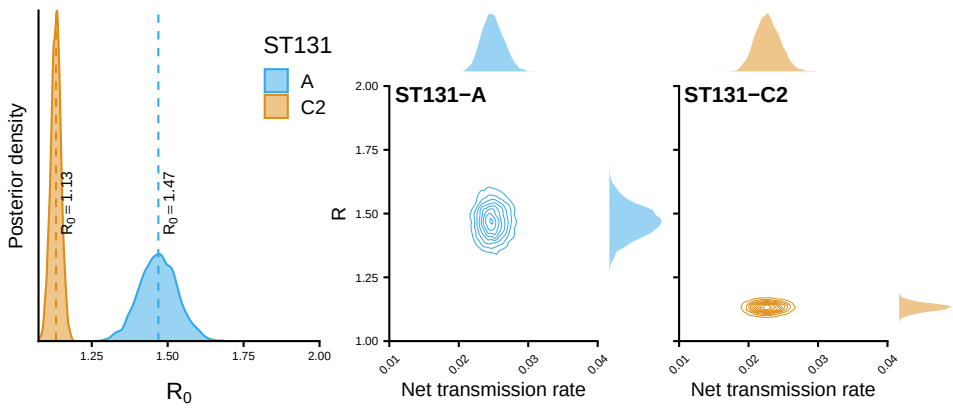

Fig. 2 The leftmost panel shows the posterior distributions of R_0 for ST131-A and ST131-C2, with median point estimate of R_0 highlighted by a dashed line. The two other panels display the joint and marginal posterior distributions of R_0 and the net transmission rate parameters for both clades.

Table 1 Mean, median and 95% credible intervals for R_0 and the net transmission rate.

	Clade A			Clade C2		
Parameter	Mean	Median	95% CI	Mean	Median	95% CI
R_0	1.47	1.47	(1.30, 1.60)	1.13	1.13	(1.08, 1.20)
Net transmission rate	0.0025	0.0025	(0.021, 0.028)	0.023	0.023	(0.019, 0.026)

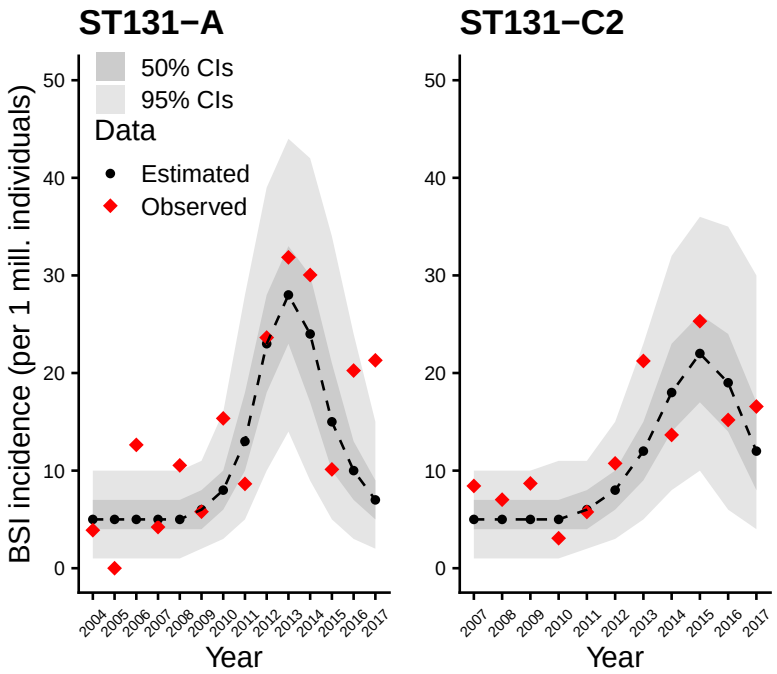

Fig. 3 Predictive fit of the model to the observed data. The red diamonds represent observed BSI counts and the black dots connected by a dashed line represent the median fit for each year.

by sampling from the posterior. These results suggest approximately ten-fold peak colonization success for ST131-A compared with ST131-C2. Of note, since the SIR model fit is intended for the calendar time window where the exponential growth of colonization success took place, these predictions should not be extrapolated into the future where the population prevalence of each clade has reached an equilibrium.

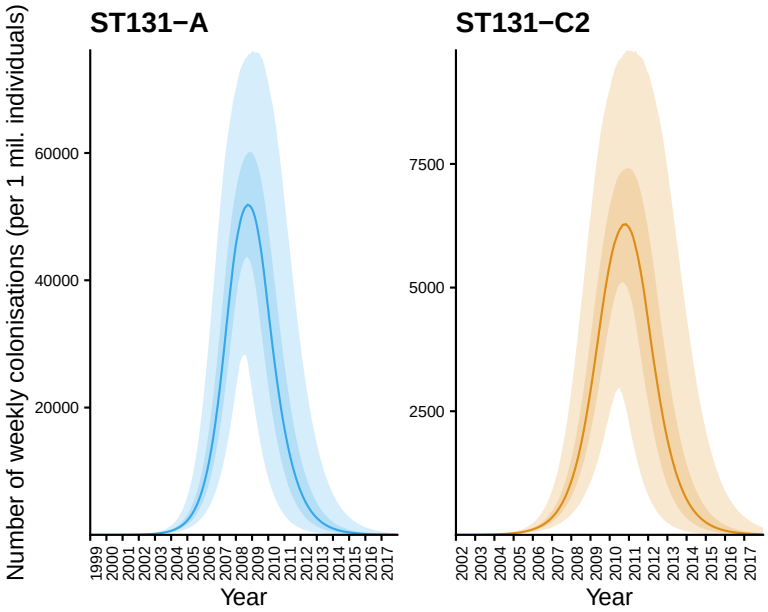

Fig. 4 Estimated median weekly colonization counts in a population of 1 000 000 individuals for ST131-A and ST131-C2. The darker and lighter shaded areas around the median line correspond to the 50% and 95% credible intervals, respectively.

3 Methods

3.1 Model and inference overview

Our modeling framework, illustrated in Figure 1, consists of two components: a *colonization model*, represented by the standard compartmental SIR (susceptible-infected-recovered) model, and an *observation model* to connect the simulated colonizations to the incidence of bloodstream infections (BSI). The specific *E. coli* clade whose dynamics is being considered is denoted by c. In the SIR-like model, the I compartment is replaced by C_c (colonization) that represents the number of individuals colonized by a clade c. The parameters of interest in the colonization model are the transmission coefficient β and the recovery rate γ. The reproduction number R_0 characterizing an expansion of a clade is defined as the ratio of β and γ:

$$R_0 = \frac{\beta}{\gamma}. \tag{1}$$

However, for inference we re-parametrize the model in terms of the basic reproduction number R_0 and the net transmission rate τ, similar to [17]. This allows us to build better interpretable priors, specifically for R_0. In addition, inference using the re-parametrized model is considerably faster due to the reduced complexity of priors required for identifiability of the model. The connection between these parameters

and β and γ are presented in Equations (1) and (2).

$$\tau = \beta - \gamma \tag{2}$$

The general challenge in inferring parameters of a colonization model is that colonization is seldom under surveillance with sufficient genomic resolution. Consequently, an observation model is needed to connect the unobserved colonization cases to the number of BSI cases, which are assumed to be observed in systematic surveillance. Taken together, the colonization and observations models then allow us to quantify the number of BSI cases that would be expected under different combinations of β and γ. We can thus infer the posterior distributions of these key parameters by identifying the β and γ such that the simulated BSI counts reproduce the observed BSI counts as accurately as possible. The model is fitted separately for the two ST131 clades of interest, A and C2, to compare their respective transmission efficiencies.

3.2 Colonization model

The SIR-like model for the colonization by clade c is defined by

$$\begin{aligned} dS_c/dt &= -\beta S_c C_c, \\ dC_c/dt &= \beta S_c C_c - \gamma C_c, \\ dR_c/dt &= \gamma C_c. \end{aligned} \tag{3}$$

The S_c compartment is the number of individuals at risk of being colonized by the clade c, while the C_c compartment is the number of individuals colonized by the clade c. The structure of the colonization model is visualized on the first row of Figure 1, where the horizontal arrows represent the flow of individuals from one compartment to the other. In practice, we discretize time and simulate transitions between compartments in steps of one week. This results in weekly counts of individuals in the different compartments, S_c^t, C_c^t, and R_c^t. Here, t indexes the week, with $t = 1, \ldots, 728$ for ST131-A, corresponding to an observation period of 14 years ($\approx 52 \times 14$ weeks), from 2004 to 2017. For ST131-C2 the observation period is 11 years from 2007 to 2017, with $t = 1, \ldots, 572$.

3.3 Observation model

The observation model for BSI connects the simulated unobserved colonization events to observed BSI cases. The observations are modeled as Poisson distributed where the mean $\bar{N}_{\text{BSI, c}}$ depends on the underlying colonization and a set of estimated parameters. Let ρ_c denote the invasiveness of the clade of interest, c, relative to the other clades:

$$\rho_c = \frac{\bar{N}_{\text{BSI, c}}}{C_c} / \frac{N_{\text{BSI,0}}}{C_0}, \tag{4}$$

where $\bar{N}_{\text{BSI, c}}$ is the mean number of BSI cases caused by clade c, $N_{\text{BSI,0}}$ is the number of BSI cases not associated with clade c, and, similarly, C_c, C_0 denote the numbers

of colonization by clade c or any other clade, respectively. In practice the quantities in (4) are defined for each week t, but the index t is here suppressed for clarity. The relative invasiveness value ρ_c is obtained from a previous study [15] (see below for details), and $N_{\text{BSI},0}$ is calculated as

$$N_{\text{BSI},0} = N\theta_{\text{BSI}} - \bar{N}_{\text{BSI, c}}, \tag{5}$$

where N is the population size, and θ_{BSI} is the estimated proportion of the population with a BSI infection in a week. As an estimate of θ_{BSI} we use the weekly average number of BSI cases across the whole study period:

$$\theta_{\text{BSI}} = \frac{n}{wN}, \tag{6}$$

where N is the population size, n is the total number of BSI infections in w weeks (728 for ST131-A and 572 for ST131-C2), obtained from the annual Norwegian national bacterial infection surveillance reports. Substituting Equations 5 and 6 into (4) and solving for $\bar{N}_{\text{BSI},c}$ yields the mean of the Poisson model

$$\bar{N}_{\text{BSI, c}} = \frac{\rho_c C_c}{(C - C_c) + \rho_c C_c} N\theta_{\text{BSI}}, \tag{7}$$

which shows how the number of colonized individuals, C_c, is connected with the mean of BSI cases, $\bar{N}_{\text{BSI, c}}$. The observed BSI cases are thus assumed to be distributed as $N_{\text{BSI, c}} \sim \text{Pois}(\bar{N}_{\text{BSI, c}})$. Some intuition for this connection can be gained by considering the special case of clade c being as invasive as all other clades, in which case $\rho_c = 1$, and (7) reduces to

$$\bar{N}_{\text{BSI},c} = \frac{C_c}{C} N\theta_{\text{BSI}}. \tag{8}$$

In this special case the mean proportion of BSI infections caused by clade c is simply equal to the proportion of colonization by clade c among all *E. coli* colonizations. Equation (7) adjusts this proportion to take into account the invasiveness of the clade c, such the proportion of infections can be larger or smaller than what is implied by the proportion of colonization. In practise we use $C = C_0 + C_c$ and assume that $C = N$, i.e., everybody in the population is colonized by some *E. coli* which is justified by considerable amount of evidence in the literature [11].

The time index t was excluded from the variables in the above definitions for simplicity, however, the observed data on BSI incidence are available as yearly aggregates. The discretized colonization model produces weekly colonization counts, so in order to compare the simulation and observations, we consequently aggregate the simulated weekly BSI counts by clade c, $N^t_{\text{BSI},c}$ into a yearly count $R^{t'}_{\text{BSI},c}$:

$$R^{t'}_{\text{BSI},c} = \sum_{t \in T_{t'}} N^t_{\text{BSI},c}, \tag{9}$$

where $T_{t'}$ is the set of all weeks in the t'-th year. As it is not plausible to assume that the population colonization process started simultaneously with the first

BSI case occurrences, we introduce a discrete random variable $\Delta \sim \mathcal{U}\{0, 5 \cdot 52\}$ that indicates the number of weeks of colonization simulation before the observed data was gathered up to five years earlier. Essentially the simulation is run for $t = -\Delta + 1, -\Delta + 2 \ldots, 728$, where $t = 1$ is the first week of the first year of data collection $t' = 2004$. This summation is repeated for each year $t' \in \{2004, \ldots, 2017\}$ for ST131-A and $t' \in \{2007, \ldots, 2017\}$ for ST131-C2.

3.4 Data

An unbiased longitudinal genomic survey of BSI isolates in Norway collected between 2002-2017 were used to estimate the incidence of ST131 clades in BSI per 1,000,000 individuals in Norway between years from 2004 to 2017 [14]. The incidence/1,000,000 for total *E. coli* BSI was available from the Norwegian Surveillence of antimicrobial resistance (NORM) reports [18]. This incidence is used to calculate the value of θ_{BSI} in (6). We previously estimated the relative invasiveness of different *E. coli* ST131 clades, specified by odds ratios that compare the frequency of each clade in geographically matched 2014-2017 neonatal gut colonization genomic data and longitudinal BSI 2003-2017 genomic data from the UK, after the emergence of ST131 and ST69 when a stable population equilibrium was reached [16], [15]. These relative invasiveness values of different *E. coli* clades were used as estimates ρ_c for the observation model.

3.5 Inference

The likelihood function is intractable for the defined hybrid deterministic-stochastic model. However, since it can be implemented efficiently as a forward simulation, we use Approximate Bayesian Computation (ABC) likelihood-free inference to calibrate the model parameters in the light of data [19].

We parametrize the model in terms of the basic reproduction number R_0 and the net transmission rate τ, similar to Lintusaari et al [17]. For R_0, we use a truncated normal prior. The underlying distribution is $N(0, 1)$ restricted to $[1.01, 3.0]$. We set priors to the parameters of the model as follows:

$$\tau \sim \mathcal{U}(0, 1), \tag{10}$$

$$R_0 \sim \psi(0, 1, 1.01, 3) \tag{11}$$

In addition to these parameters that define the colonization model, we include the parameter Δ describes the delay between colonization and onset of infection. We assign Δ a uniform prior, allowing for a delay between 0 and 5 years. Given that the unit of Δ is one week, the upper limit of the uniform distribution equals 260 weeks.

$$\Delta \sim \mathcal{U}(0, 260) \tag{12}$$

Since Δ operates on a markedly different scale from τ and R_0, we scale it by 0.0001 before fitting the model and then transform it back to the original scale for interpretation of the results.

To use ABC, following operational quantities are needed: 1) summary statistics to sufficiently reduce the dimension of the data, 2) a discrepancy function that allows comparing the simulated synthetic data summaries with the summaries of the observed data, and 3) a threshold parameter that reflects tolerable error between the summarized synthetic and observed data, to accept the parameter that generated the simulation as a draw from the posterior. We constructed three summary statistics, S_1, S_2, S_3, to compare how the observed and simulated BSI incidences evolve in time. S_1 is defined as the maximum BSI incidence over the years within the interval $[2004, 2017]$ for ST131-A and $[2007, 2017]$ for ST131-C2. S_2 is the number of years from the beginning of the simulation (year 2004 for ST131-A and 2007 for ST131-C2) to the maximum BSI incidence. S_3 is the BSI incidence at the beginning of the observation period. We apply $\log(x + 0.5)$-transformation on the summaries S_1 and S_3 because the scale of these BSI count -based summaries, which can vary between 0 and 1,000,000 (population size used in the simulation), is very different from the scale of the peaking time summary S_2 (ranging between 1 and 11 or 14 years). Finally, the Euclidean distance was used to compare the observed and simulated data summaries.

Using sequential Monte Carlo (SMC) ABC [20], we obtained 10,000 samples as an approximation to the posterior distribution, with the following sequence of decreasing thresholds: $[1.0, 0.5, 0.35, 0.1]$. The convergence of the algorithm over these populations is visualized in Figure 5. At the post-processing stage, the posteriors were resampled using the obtained weights. We used the ELFI implementation of the SMC ABC algorithm [21]. The model was fitted separately for clades A and C2 using a Python implementation of the simulator model and the ABC inference pipeline available in the open-source likelihood-free inference software package, Engine for Likelihood-free Inference (ELFI) [22]. The complete analysis pipeline written in Python is available in GitHub at (https://github.com/fanoja/Ecoli-R0).

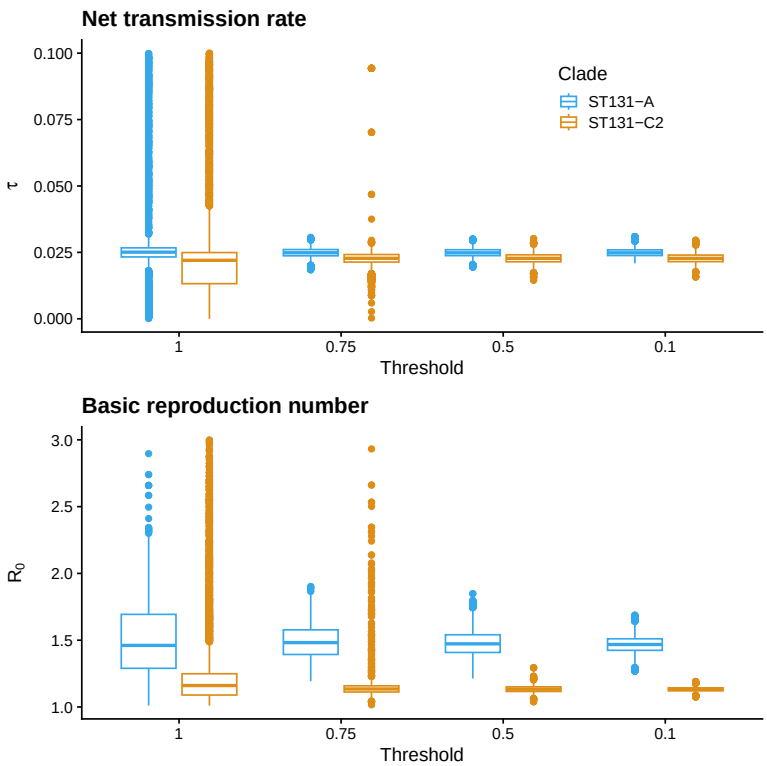

Fig. 5 Convergence of SMC ABC for net transmission rate τ and basic reproduction number R_0. The figure contains four SMC populations with thresholds 1, 0.75, 0.5 and 0.1 for ST131-A and ST131-C2.

4 Discussion

While R_0 represents a key epidemiological characteristic that is typically rapidly inferred for emerging pathogenic viruses, its quantification has remained far more elusive for pathogenic bacteria causing opportunistic infections. The primary reasons behind this difficulty are the lack of systematic high-resolution surveillance of asymptomatic colonization rates for almost any bacterial species, the temporal lag with which infection cases tend to occur, and the need to have a system in place for whole-genome sequencing of infection isolates from sufficiently representative surveillance. Here we were able to fill this knowledge gap by combining systematic population genomics based surveillance of *E. coli* bloodstream infection isolates in both Norway and the UK, with demographics and annual national-level mandatory reporting statistics of these infections in Norway. Furthermore, we had the opportunity to use recently estimated odds ratios for each considered clade of *E. coli* [16], which compare the frequency of asymptomatic colonization to the frequency of bloodstream infection in a temporally matched host population in the UK.

By using all the above-mentioned data sources, we built a hybrid deterministic-stochastic model that first simulates the asymptomatic spread of a novel bacterial clone in a population and then feeds this information into an observation model that generates infection cases at the desired temporal resolution. Unlike the basic epidemiological models, our approach results in an intractable likelihood, calling for simulator-based inference methods, such as ABC [19], to calibrate the model parameters. Recently, Pesonen et al. demonstrated the extended possibilities offered by ABC inference for simulator-based modelling of R_0 when the transmission process exhibits latent heterogeneity [23], using a model derived for the Ebola virus by Britton and Tomba [24]. Despite our focus on *E. coli*, we believe that the current study can serve as a proof-of-concept for modelling expansions of other bacteria with pathogenic potential and thus extend the reach of infectious disease epidemiology to further novel applications.

Compartmental models for transmission studies are generally built from assumptions that might not hold in reality, such as homogeneous mixing of host population, mass action incidence to determine rate of new infections, effective contacts (contact always leads to successful transmission) and unchanging demographics on the relevant timescale [25]. Despite these simplifying assumptions, even basic compartmental models have been widely popular and successfully used for a large number of studies in infectious disease epidemiology.

An alternative compartmental model for bacterial colonization of the type we consider here would be the SIS model [25]. Here, re-colonization of the same individual is possible and there is no resistance acquired against colonization, leading to exclusion of the recovered compartment. However, since we are operating on relatively short timescales of a few years at a national level, using an SIR-like colonization model is considered to be a reasonable approximation to the underlying transmission chains across the host population. We did not include any explicit age structure in our model, although its use could be motivated by the higher incidence of BSI in the elderly population. Nevertheless, it is justifiable to consider that the expanding clades are equally capable of colonizing hosts irrespective of their age, translating to model fits where the relative difference between the clades is robustly quantified. To better capture the variability in incidence at the beginning of the clade expansion, a stochastic branching process based on contact networks could be used in future work in addition to the deterministic compartmental model [25]. Despite the deterministic nature of the SIR-like model for colonization our results show a reasonable degree of fit both in the earliest phase of expansion and during he peaking incidence (Figure 3).

Our results indicate a much higher R_0 for clade A (posterior mean 1.47) compared with clade C2 (posterior mean 1.13), which translates to a markedly higher transmission efficiency of A that is comparable to some pandemic influenza strains such as the 2009 H1N1 [26]. This is well aligned with the earlier Bayesian phylodynamic inference based finding of significantly higher increase in the effective population size of A clade during the mid-2000s [14]. The significantly lower estimated transmissibility of ST131-C2 suggests that its global dissemination has been substantially aided by

antibiotic selection pressure and that it may be more effectively transmitted through health care facilities instead of primarily community driven transmission. For further discussion on the drivers of clade C2 equilibrium prevalence in a population, see [16]. Importantly, these two clades of the ST131 clone have diverged very recently and are still closely related in terms of their core genomes [14, 27, 28]. It is thus remarkable how different they are in terms of their estimated ability to colonize new hosts, which highlights the need for further research on whether this difference can be explained by subtle genetic diversity in their core genomes, such as in metabolic capacity, or by variable accessory genome content (or both). These topics have been a subject of intensive recent research efforts in *E. coli* [27–33], but thus far no clear conclusions have been reached concerning main genetic drivers underlying phenotypic variation at this level of relatedness. Improved *in vitro* and *in vivo* experiments combined with high-resolution comparative population genomics and further modelling could thus offer a promising strategy towards resolving the likely polygenic basis of the estimated difference in transmission efficiency.

Acknowledgements. Research in this publication was supported by the Research Council of Norway through its Centre of Excellence Integreat - The Norwegian Centre for knowledge-driven machine learning, project number 332645, Trond Mohn Foundation (BATTALION grant) and Academy of Finland (EuroHPC grant, Flagship programme: Finnish Center for Artificial Intelligence FCAI, and grants 358246, 352986) and EU (H2020 grant 101016775 and NextGenerationEU). Fanni Ojala acknowledges travel support from the European Union's Horizon 2020 research and innovation programme under ELISE Grant Agreement No 951847.

Declarations

Data and analysis code are available at https://github.com/fanoja/Ecoli-R0.

References

[1] Dietz, K.: The estimation of the basic reproduction number for infectious diseases. http://dx.doi.org/10.1177/096228029300200103 **2**, 23–41 (1993) https://doi.org/10.1177/096228029300200103

[2] Heffernan, J.M., Smith, R.J., Wahl, L.M.: Perspectives on the basic reproductive ratio. Journal of The Royal Society Interface **2**, 281–293 (2005) https://doi.org/10.1098/RSIF.2005.0042

[3] O'Driscoll, M., Harry, C., Donnelly, C.A., Cori, A., Dorigatti, I.: A comparative analysis of statistical methods to estimate the reproduction number in emerging epidemics, with implications for the current coronavirus disease 2019 (covid-19) pandemic. Clinical Infectious Diseases **73**, 215–223 (2021) https://doi.org/10.1093/CID/CIAA1599

[4] Ali, W., Overton, C.E., Wilkinson, R.R., Sharkey, K.J.: Deterministic epidemic models overestimate the basic reproduction number of observed outbreaks. Infectious Disease Modelling (2024) https://doi.org/10.1016/J.IDM.2024.02.007

[5] Delamater, P.L., Street, E.J., Leslie, T.F., Yang, Y.T., Jacobsen, K.H.: Complexity of the basic reproduction number (r0). Emerging Infectious Diseases **25**, 1 (2019) https://doi.org/10.3201/EID2501.171901

[6] Presti, A.L., Vacca, P., Neri, A., Fazio, C., Ambrosio, L., Rezza, G., Stefanelli, P.: Estimates of the reproductive numbers and demographic reconstruction of outbreak associated with c:p1.5–1,10–8:f3–6:st–11(cc11) neisseria meningitidis strains. Infection, Genetics and Evolution **84**, 104360 (2020) https://doi.org/10.1016/J.MEEGID.2020.104360

[7] Ma, Y., Horsburgh, C.R., White, L.F., Jenkins, H.E.: Quantifying tb transmission: a systematic review of reproduction number and serial interval estimates for tuberculosis. Epidemiology Infection **146**, 1478–1494 (2018) https://doi.org/10.1017/S0950268818001760

[8] Laegreid, W.W., Keen, J.E.: Estimation of the basic reproduction ratio (r0) for shiga toxin-producing escherichia coli o157:h7 (stec o157) in beef calves. Epidemiology Infection **132**, 291–295 (2004) https://doi.org/10.1017/S0950268803001705

[9] Henderson, A., Nimmo, G.R.: Control of healthcare- and community-associated mrsa: recent progress and persisting challenges. British Medical Bulletin **125**, 25–41 (2018) https://doi.org/10.1093/BMB/LDX046

[10] Hal, S.J., Willems, R.J.L., Gouliouris, T., Ballard, S.A., Coque, T.M., Hammerum, A.M., Hegstad, K., Pinholt, M., Howden, B.P., Malhotra-Kumar, S., Werner, G., Yanagihara, K., Earl, A.M., Raven, K.E., Corander, J., Bowden, R.: The interplay between community and hospital enterococcus faecium clones within health-care settings: a genomic analysis. The Lancet Microbe **3**, 133–141 (2022) https://doi.org/10.1016/S2666-5247(21)00236-6

[11] Donnenberg, M.: Escherichia Coli: Pathotypes and Principles of Pathogenesis, Edition 2, 2nd edn. Academic Press, New York (2013)

[12] Riley, L.W.: Pandemic lineages of extraintestinal pathogenic escherichia coli. Clinical microbiology and infection : the official publication of the European Society of Clinical Microbiology and Infectious Diseases **20**, 380–390 (2014) https://doi.org/10.1111/1469-0691.12646

[13] Pitout, J.D.D., Peirano, G., Chen, L., DeVinney, R., Matsumura, Y.: Escherichia coli st1193: Following in the footsteps of e. coli st131. Antimicrobial agents and chemotherapy **66** (2022) https://doi.org/10.1128/AAC.00511-22

[14] Gladstone, R.A., McNally, A., Pöntinen, A.K., Tonkin-Hill, G., Lees, J.A., Skytén, K., Cléon, F., Christensen, M.O.K., Haldorsen, B.C., Bye, K.K., Gammelsrud, K.W., Hjetland, R., Kümmel, A., Larsen, H.E., Lindemann, P.C., Löhr, I.H., Marvik, Nilsen, E., Noer, M.T., Simonsen, G.S., Steinbakk, M., Tofteland, S., Vattøy, M., Bentley, S.D., Croucher, N.J., Parkhill, J., Johnsen, P.J., Samuelsen, Corander, J.: Emergence and dissemination of antimicrobial resistance in escherichia coli causing bloodstream infections in norway in 2002–17: a nationwide, longitudinal, microbial population genomic study. The Lancet Microbe **2**, 331–341 (2021) https://doi.org/10.1016/S2666-5247(21)00031-8

[15] Mäklin, T., Thorpe, H.A., Pöntinen, A.K., Gladstone, R.A., Shao, Y., Pesonen, M., McNally, A., Johnsen, P.J., Samuelsen, Lawley, T.D., Honkela, A., Corander, J.: Strong pathogen competition in neonatal gut colonisation. Nature Communications 2022 13:1 **13**, 1–13 (2022) https://doi.org/10.1038/s41467-022-35178-5

[16] Pöntinen, A.K., Gladstone, R.A., Pesonen, H., Pesonen, M., Cléon, F., Parcell, B.J., Kallonen, T., Simonsen, G.S., Croucher, N.J., McNally, A., Parkhill, J., Johnsen, P.J., Samuelsen, Corander, J.: Modulation of multidrug-resistant clone success in escherichia coli populations: a longitudinal, multi-country, genomic and antibiotic usage cohort study. The Lancet Microbe **5**, 142–150 (2024) https://doi.org/10.1016/S2666-5247(23)00292-6

[17] Lintusaari, J., Blomstedt, P., Rose, B., Sivula, T., Gutmann, M.U., Kaski, S., Corander, J., Gascuel, O., Zhukova, A., Beaumont, M.: Resolving outbreak dynamics using approximate bayesian computation for stochastic birth–death models. Wellcome Open Research 2019 4:14 **4**, 14 (2019) https://doi.org/10.12688/wellcomeopenres.15048.2

[18] Nord-Norge, U.: NORM - Norsk overvåkingssystem for antibiotikaresistens hos mikrober. https://www.unn.no/fag-og-forskning/norm-norsk-overvakingssystem-for-antibiotikaresistens-hos-mikrober#rapporter

[19] Lintusaari, J., Gutmann, M.U., Dutta, R., Kaski, S., Corander, J.: Fundamentals and recent developments in approximate bayesian computation. Systematic Biology **66**, 66–82 (2017) https://doi.org/10.1093/SYSBIO/SYW077

[20] Filippi, S., Barnes, C.P., Cornebise, J., Stumpf, M.P.H.: On optimality of kernels for approximate bayesian computation using sequential monte carlo. Statistical Applications in Genetics and Molecular Biology **12**, 87–107 (2013) https://doi.org/10.1515/SAGMB-2012-0069/MACHINEREADABLECITATION/RIS

[21] API — ELFI 0.8.7 documentation. https://elfi.readthedocs.io/en/latest/api.html#elfi.SMC

[22] Lintusaari, J., Vuollekoski, H., Kangasrääsiö, A., Skytén, K., Järvenpää, M., Marttinen, P., Gutmann, M.U., Vehtari, A., Corander, J., Kaski, S.: Elfi: Engine for likelihood-free inference. Journal of Machine Learning Research **19**, 1–7 (2018)

[23] Pesonen, H., Simola, U., Köhn-Luque, A., Vuollekoski, H., Lai, X., Frigessi, A., Kaski, S., Frazier, D.T., Maneesoonthorn, W., Martin, G.M., Corander, J.: Abc of the future. International Statistical Review **91**, 243–268 (2023) https://doi.org/10.1111/insr.12522

[24] Britton, T., Tomba, G.S.: Estimation in emerging epidemics: biases and remedies. Journal of the Royal Society Interface **16** (2019) https://doi.org/10.1098/RSIF.2018.0670

[25] Brauer, F., Castillo-Chavez, C., Feng, Z.: Mathematical Models in Epidemiology. Springer, New York (2019)

[26] Cheung, J.T.L., Tsang, T.K., Yen, H.L., Perera, R.A.P.M., Mok, C.K.P., Lin, Y.P., Cowling, B.J., Peiris, M.: Determining existing human population immunity as part of assessing influenza pandemic risk - volume 28, number 5—may 2022 - emerging infectious diseases journal - cdc. Emerging Infectious Diseases **28**, 977–985 (2022) https://doi.org/10.3201/EID2805.211965

[27] McNally, A., Oren, Y., Kelly, D., Pascoe, B., Dunn, S., Sreecharan, T., Vehkala, M., Välimäki, N., Prentice, M.B., Ashour, A., Avram, O., Pupko, T., Dobrindt, U., Literak, I., Guenther, S., Schaufler, K., Wieler, L.H., Zhiyong, Z., Sheppard, S.K., McInerney, J.O., Corander, J.: Combined analysis of variation in core, accessory and regulatory genome regions provides a super-resolution view into the evolution of bacterial populations. PLoS Genetics **12** (2016) https://doi.org/10.1371/journal.pgen.1006280

[28] McNally, A., Kallonen, T., Connor, C., Abudahab, K., Aanensen, D.M., Horner, C., Peacock, S.J., Parkhill, J., Croucher, N.J., Corander, J.: Diversification of colonization factors in a multidrug-resistant escherichia coli lineage evolving under negative frequency- dependent selection. mBio **10** (2019) https://doi.org/10.1128/mBio.00644-19

[29] Connor, C.H., Zucoloto, A.Z., Munnoch, J.T., Yu, I.L., Corander, J., Hoskisson, P.A., McDonald, B., McNally, A.: Multidrug-resistant e. coli encoding high genetic diversity in carbohydrate metabolism genes displace commensal e. coli from the intestinal tract. PLoS Biology **21** (2023) https://doi.org/10.1371/journal.pbio.3002329

[30] Hall, R.J., Whelan, F.J., Cummins, E.A., Connor, C., McNally, A., McInerney, J.O.: Gene-gene relationships in an escherichia coli accessory genome are linked to function and mobility. Microbial Genomics **7** (2021) https://doi.org/10.1099/MGEN.0.000650

[31] Cummins, E.A., Hall, R.J., Connor, C., McInerney, J.O., McNally, A.: Distinct evolutionary trajectories in the escherichia coli pangenome occur within sequence types. Microbial Genomics **8**, 000903 (2022) https://doi.org/10.1099/MGEN.0.000903/CITE/REFWORKS

[32] Rousset, F., Cabezas-Caballero, J., Piastra-Facon, F., Fernández-Rodríguez, J., Clermont, O., Denamur, E., Rocha, E.P.C., Bikard, D.: The impact of genetic diversity on gene essentiality within the escherichia coli species. Nature Microbiology 2021 6:3 **6**, 301–312 (2021) https://doi.org/10.1038/s41564-020-00839-y

[33] Micaletto, M., Fleurier, S., Dion, S., Denamur, E., Matic, I.: The protein carboxymethyltransferase–dependent aspartate salvage pathway plays a crucial role in the intricate metabolic network of escherichia coli. Science Advances **10**, 767 (2024) https://doi.org/10.1126/SCIADV.ADJ0767/SUPPL_FILE/SCIADV.ADJ0767_SM.PDF